Geosci. Model Dev. Discuss., 8, 3197–3218, 2015
www.geosci-model-dev-discuss.net/8/3197/2015/
doi:10.5194/gmdd-8-3197-2015

Geoscientific Model Development Discussions
Open Access

Representation of vegetation effects on the snow-covered albedo in the Noah land surface model with multiple physics options

S. Park[1,3,4] and S. K. Park[1,2,3,4]

[1]Department of Atmospheric Science and Engineering, Ewha Womans University, Seoul, Republic of Korea
[2]Department of Environmental Science and Engineering, Ewha Womans University, Seoul, Republic of Korea
[3]Center for Climate/Environment Change Prediction Research, Ewha Womans University, Seoul, Republic of Korea
[4]Severe Storm Research Center, Ewha Womans University, Seoul, Republic of Korea

Received: 6 February 2015 – Accepted: 9 March 2015 – Published: 13 April 2015

Correspondence to: S. K. Park (spark@ewha.ac.kr)

Published by Copernicus Publications on behalf of the European Geosciences Union.

Representation of vegetation effects on the snow-covered albedo

S. Park and S. K. Park

Abstract

Snow albedo plays a critical role in calculating the energy budget, but parameterization of the snow surface albedo is still under great uncertainty. It varies with snow grain size, snow cover thickness, snow age, forest shading factor and other variables. Snow albedo of forest is typically lower than that of short vegetation; thus snow albedo is dependent on the spatial distributions of characteristic land cover and on the canopy density and structure. In the Noah land surface model with multiple physics options (Noah-MP), almost all vegetation types in East Asia during winter have the minimum values of leaf area index (LAI) and stem area index (SAI), which are too low and do not consider the vegetation types. Because LAI and SAI are represented in terms of photosynthetic activeness, the vegetation effect rarely exerts on the surface albedo in winter in East Asia with only these parameters. Thus, we investigated the vegetation effects on the snow-covered albedo from observations and evaluated the model improvement by considering such effect. We found that calculation of albedo without proper reflection of the vegetation effect is mainly responsible for the large positive bias in winter. Therefore, we developed new parameters, called leaf index (LI) and stem index (SI), which properly manage the effect of vegetation structure on the winter albedo. As a result, the Noah-MP's performance in albedo has been significantly improved – RMSE is reduced by approximately 73 %.

1 Introduction

Snow albedo is very important when it comes to calculating the energy budget at the land surface, but the vegetation effects on adequate parameterization of the snow surface albedo are still under great uncertainty. Vegetation influences both snow cover and albedo, which can be summarized in three points. First, the canopy changes snow depth because leaves and branches can intercept part of the snow. Second, vegetation generally has a larger roughness than bare soil. Normally just a small amount

GMDD

8, 3197–3218, 2015

of snow is sufficient to cover a bare soil, resulting in high albedo. However, the same snow amount above a grass field cannot cover all the grass because some individual elements of grass can be higher than snow depth. Thus, in case of snow, total albedo over a grass is lower than that over a bare soil. With the same amount of snow, total albedo becomes much lower over a forest. For example, in order to fully cover a tree whose height is 10 m, snow should be accumulated more than 10 m. Although the tree top can be intercepted by snow with the accumulated amount lower than 10 m, the shading effect of tree through its structure still remains at off-nadir solar zenith angle. Lastly, vegetation can change heat flux with different temperature from a bare soil. Moreover, vegetation changes the longwave radiation as a tree re-emits radiation downwards. Although the air temperature is just below 0 °C, there is no frost under trees and snow melts earlier.

Previous studies have addressed the apparent relationship between snow cover over different vegetation types and the snow surface albedo through field measurements and satellite observations as well (Henderson-Sellers and Wilson, 1983; Jin et al., 2002; Gao et al., 2005). Gao et al. (2005) found that the maximum snow-covered albedos of non-forest types are typically higher than those of forest types, showing the shading effect of the density and vertical structure of canopy on snow cover. Forest shading is caused by leaves, stems, branches and trunks, and has a direct effect on albedo. Despite a spatial distribution of albedo generally follows the patterns of land cover type (Jin et al., 2002), many land surface models (LSMs) do not consider the vegetation effect on snow albedo or use impractical vegetation parameters (Essery, 2013). In numerical models, albedo under snow condition is usually parameterized through separate treatments for different surfaces (i.e., snow-covered vs. snow-free), which are weighted by the snow cover fraction. Thus, the snow cover fraction is also important for accurate calculation of albedo.

In this study, we examine how vegetation effects can be adequately considered for computation of albedo during winter in the Noah land surface model with multiple physics options (Noah-MP) (Niu et al., 2011; Yang et al., 2011). In the Noah-MP, the

GMDD
8, 3197–3218, 2015

formula for albedo includes a sum of leaf area index (LAI) and stem area index (SAI). The grid box values of LAI and SAI in winter are set to the same minimum values over all vegetation types and are too low. The crucial point to note is that both LAI and SAI are represented as photosynthetically active structures in the Noah-MP. With only photosynthetically active leaves and stems in winter, the model cannot simulate albedo accurately due to a deficiency in the effect of nonphotosynthetic vegetation structures. They also cast a shadow on the snow-covered surface by the canopy, arising from the solar zenith angle (SZA). Such a deficiency can be a major cause of the large positive bias errors of albedo in the Noah-MP. Therefore, we improve the model-calculated albedo through a clear understanding of vegetation effects on albedo.

2 Model and data description

2.1 The Noah-MP

The Noah-MP has evolved from the Noah land surface model and has a variety of potentials to expedite physically based ensemble climate predictions and identification of both the optimal scheme combinations and the critical processes controlling the coupling strength (Niu et al., 2011). In this study, the model has been used in an offline mode, simulating the land surface processes with atmospheric forcing. The Noah-MP has 12 different scheme sets representing various physical processes. We select the default options that were verified for the global river basins in Yang et al. (2011). For this study, we have only changed the option of snow surface albedo scheme from the Canadian Land Surface Scheme (CLASS; Verseghy, 1991) to the Biosphere–Atmosphere Transfer Scheme (BATS; Dickinson et al., 1993; Yang et al., 1997). In contrast to the CLASS which simply computes the overall snow albedo with fresh snow albedo and snow age, the BATS calculates snow albedo for direct and diffuse radiation in visible and near-infrared broadband accounting for several aspects such as fresh snow

GMDD
8, 3197–3218, 2015

albedo, snow age, grain size growth, impurity, and especially solar zenith angle (SZA) (Niu et al., 2011).

The computational domain covers 4000 km × 4000 km, with a grid size of approximately 30 km, in the East Asia region (105–145° E, 20–60° N). However, most analyses are conducted in north of 40° N where snow falls moderately. The model runs during the years 2001–2010 with a spin-up time of 6 months.

2.2 Data sets

2.2.1 Atmospheric forcing

The atmospheric data is required to force the land surface processes in LSMs. For the Noah-MP, the Global Land Data Assimilation System (GLDAS) (Rodell et al., 2004) data have been used to drive the model during the period 2001–2010. The atmospheric forcing fields can be obtained from the atmospheric data assimilation system (ADAS) component of a weather forecast and analysis system or from a reanalysis fields. The data consist of 8 forcing fields: precipitation, downward shortwave and longwave radiation, near-surface air temperature, near-surface specific humidity, near-surface zonal and meridional wind, and surface pressure. The temporal resolution is 3 h and the spatial resolution is 0.25°.

2.2.2 MODIS albedo

The MODerate-resolution Imaging Spectroradiometer (MODIS) albedo product (MCD43C3) is produced every 16 days in a level-3 data set, projected to a 0.05 latitude/longitude Climate Modelling Grid (CMG) (Schaaf et al., 2002). We use total shortwave broadband for white-sky albedo (or bihemispherical reflectance under conditions of isotropic illumination) and quality flags that include the percentage of snow and the percentage contribution of fine resolution data. The albedo products were evaluated by in situ measurement (Cescatti et al., 2012).

2.2.3 USGS land use and land cover

The yearly MODIS land cover and land use data within the International Geosphere–Biosphere Programme (IGBP) global vegetation classification scheme is slightly modified to fit into the land cover classification of the U.S. Geological Survey (USGS) (Anderson et al., 1976). Land cover types are grouped into 27 types according to the USGS classification (see Table 1).

3 Results

3.1 Physical properties of snow-covered vegetation

For figuring out the difference of albedo among various vegetation types, we select 10 areas within 40–60° N (Fig. 1) where a single type or similar two types of vegetation occupies more than 70 % in each area (Table 2). In order to minimize the effects of snow cover change, we have averaged the white-sky albedo over dominating vegetation type in each area for winter time (i.e., 273–129 as Julian day) in total shortwave broadband during 10 years (2001–2010) with a 100 % snow cover fraction (SCF) (see Fig. 2). It is evident that the snow-covered albedo values are distributed over a wide range and relatively low for various forest types. The snow-covered surface albedo is different when the snow is over the ground surface vs. over the canopy, mainly due to an uneven structure of the canopy and the forest shading effect. When the growing season is over, leaves and stems are mostly shed and their amount remains unchanged – reaching the minimum values. These values may be different according to vegetation type, thus making distinctions of albedos over the forest types.

Compared to the observation as shown in Fig. 2, the Noah-MP snow-covered albedos are overestimated over all vegetation types in winter and have little difference between forest and short vegetation (not shown). This is mainly due to the use of LAI and SAI, which are not able to quantify leaves and stems representing the forest masking in winter. In the Noah-MP, LAI and SAI are computed as follows:

$$\mathrm{LAI} = \max(m_{\mathrm{leaf}} \times \mathrm{LAPM}, \mathrm{LAI}_{\mathrm{min}}) \quad (1)$$

$$\mathrm{SAI} = \max(m_{\mathrm{stem}} \times \mathrm{SAPM}, \mathrm{SAI}_{\mathrm{min}}) \quad (2)$$

where m_{leaf} (m_{stem}) is the leaf (stem) mass (in $\mathrm{g\,m^{-2}}$) and LAPM (SAPM) is the leaf (stem) area per unit mass (in $\mathrm{m^2\,g^{-1}}$). The subscript "min" implies the minimum value. The default value of $\mathrm{LAI}_{\mathrm{min}}$ and $\mathrm{SAI}_{\mathrm{min}}$ is 0.05 and 0.01 $\mathrm{m^2\,m^{-2}}$, respectively, and the effect of different vegetation types is not considered. During most of the winter period, both LAI and SAI are set to the minimum values (i.e., $\mathrm{LAI}_{\mathrm{min}}$ and $\mathrm{SAI}_{\mathrm{min}}$). Tian et al. (2004) indicated that discrepancies in the winter albedos between the MODIS observation and LSMs were related to the uncertainty in quantifying LAI and SAI in the model. They also mentioned that stems would have different single-scattering albedo than green leaves, and hence it might be inadequate for the model to treat LAI and SAI the same in the albedo parameterization.

As previously stated, both LAI and SAI are linked to photosynthetic activeness in the Noah-MP. Compared to the reference value of $\mathrm{LAI}_{\mathrm{min}}$ (e.g., Asner et al., 2003), the model-calculated $\mathrm{LAI}_{\mathrm{min}}$ is highly underestimated for all forest types during a winter season, and $\mathrm{SAI}_{\mathrm{min}}$ is much lower than $\mathrm{LAI}_{\mathrm{min}}$. These uncertainties are caused by their definition. Actually, the structure and density of all leaves and stems have effects on albedo. Observed LAI includes all leaves, regardless of the ability to express photosynthesis; hence it is higher than the model calculation. Therefore, it is necessary to properly parameterize the vegetation effects on the snow-covered albedo.

3.2 Parameterization of the vegetation effects on the snow surface albedo

We introduce new parameters – leaf index (LI) and stem index (SI). LI represents a sum of LAI defined in the Noah-MP (i.e., photosynthetic leaves) and LAI of nonphotosynthetic leaves. We substitute LI with the reference minimum values (see Asner et al., 2003) for four forest types as given in Table 3 in Sect. 3.2.2 in order to draw realistic

GMDD
8, 3197–3218, 2015

Representation of vegetation effects on the snow-covered albedo

S. Park and S. K. Park

SI effect. SI represents a sum of SAI defined in the model (i.e., photosynthetic stems) and SAI of nonphotosynthetic stems. To figure out how albedo responses to stems, we examine the sensitivity of winter albedo to SI over forest types in the Noah-MP and then validate albedo with the optimal SI value.

3.2.1 Sensitivity of the snow-covered albedo to SI

We focus on the snow-covered albedo treatments rather than running the model with full physics in idealized cases. To avoid the effects of other parameters such as snow cover fraction and snow age, we assume a fresh snow with the snow cover fraction set to 1, the wetted fraction of both LI and SI to 1, and snow depth to 1 m. SI varies from 0.1 to 10.0 with an interval of 0.1 having a SZA of 0, 30, 45, 60 and 75°. In the Noah-MP, options for two-stream radiation transfer decide the values of canopy gap probability for direct and diffuse beam. Here the canopy gap probability is defined as the chance that a photon penetrates through the vegetation without being intercepted by any crowns (Niu and Yang, 2004). The modified two-stream approximation (MTSA), which is the first option of the two-stream radiation transfer scheme, explicitly includes the three-dimensional structure of the vegetation canopy by calculating the total canopy gap probability for direct beam, P_c. It equals to the sum of the between-crown gap probability, P_{bc}, which is a function of crown geometric properties and the SZA, and the within-crown gap probability, P_{wc}, which is parameterized on the basis of a modified version of Beer's law:

$$P_{bc} = e^{-\rho_t \pi R^2 / \cos(\theta')} \tag{3}$$

$$P_{wc} = (1 - P_{bc}) e^{-0.5 F_a H_d / \cos\theta} \tag{4}$$

$$P_c = \min(1 - f_{veg}, P_{bc} + P_{wc}) \tag{5}$$

where ρ_t is the crown density (stems m^{-2}), R is the horizontal crown radius, θ is the solar zenith angle, $\theta' = \tan^{-1}[(b/R)\tan\theta]$, and b is the vertical crown radius. F_a is the foliage area volume density (m^{-1}) and is equal to $\mathrm{LSAI}/(\frac{4}{3}\pi R^2 b \rho_t)$, where LSAI is the

GMDD
8, 3197–3218, 2015

effective leaf and stem area index, through which the effect of clumping of needles into shoots is included (Chen et al., 1991; Niu and Yang, 2004). H_d is the crown depth. f_{veg} is the green vegetation fraction ranged from zero to 1. Therefore, if we apply new LI and SI, LSAI is changed and then the canopy gap probability is changed.

Figure 3 depicts the sensitivity of the snow-covered surface albedo and each term in albedo equation in the Noah-MP to SI averaged over four forest types for different SZA. Total albedo by vegetation and ground, f_{re}, is

$$f_{re} = \begin{cases} \alpha_{dc}(1 - P_c) + \alpha_d P_c & \text{(for direct beam)} \\ \alpha_{ic}(1 - K_{open}) + \alpha_i K_{open} & \text{(for diffuse beam)} \end{cases} \tag{6}$$

where α_d and α_{dc} is the direct albedo of the underlying surface and canopy, respectively, and α_i and α_{ic} is the diffuse albedo of the underlying surface and canopy, respectively. How to calculate canopy albedo is explained in detail in Sellers (1985). K_{open} is the between-crown gap probability for diffuse radiation. Here, K_{open} is set to 0.05.

As expected, total albedo over four forest types generally decreases with SI because snow albedo over the vegetated surface is lower than that over the bare soil surface (Fig. 3a). At a fixed SI, albedo represents different patterns for different SZA – albedo increases (decreases) with increasing SZA at relatively high (low) SI. Note that there is sufficient ground surface at relatively low SI that can be shaded by the vegetative canopy as SZA increases (Fig. 3b). Thus, at low SI, albedo is highest when the shadow area of underlying snow-covered surface is the smallest, that is, at local noon. Wang and Zeng (2010) also pointed out this feature using the Community Land Model 3.0. Canopy albedo also decreases with SI due to the increasing optical depth of direct and diffuse beam through leaf and stem area (Fig. 3c–f).

3.2.2 Validation of surface albedo with the optimal SI value

For quantifying the forest shading effect through SI in winter, we compare the Noah-MP albedo with observation. We performed model runs repeatedly by changing SI from 0.0

GMDD
8, 3197–3218, 2015

to 3.0 in order to find the optimal SI for each forest type that reduce a bias of albedo between observation and model output. LAI and SAI were used to calculate carbon flux as well as radiation during the growing season. Hence, we have applied LI and SI when the growing season index was off. Albedo is averaged for 10 years in specific winter days (i.e. 337, 353, and 1, 17, and 33 as Julian day) for vegetation types in the East Asia region. Figure 4 shows the bias errors of albedo between observation and model output (i.e., absolute values of model minus observation) with SI values for four forest types (i.e., deciduous broadleaf, deciduous needleleaf, evergreen needleleaf and mixed forest) and three short vegetation types (i.e., grassland, shrubland and mixed shrubland/grassland). In case of forest types, the bias errors of albedo decrease with increasing SI. On the contrary, the bias errors of albedo for short vegetation types decrease slightly or even increase with increasing SI. It does not make sense that short vegetation has high SI; therefore modification of albedo over short vegetation by increasing SI is meaningless. The optimized SI values, effective for reduction of bias errors in albedo, are 1.3 for deciduous broadleaf forest, 1.5 for deciduous needleleaf forest, 2.3 for evergreen needleleaf forest, and 2.0 for mixed forest (see Table 3). The bias errors of albedo rarely decrease when SI reaches a certain value. Therefore, when the difference of bias between two consecutive SI is below 0.005, SI is considered to be optimized. The other land cover types are not optimized and the default values of SAI_{min} are used. The reason why the errors do not decrease below a certain level is possibly due to other parameters such as snow age, fresh snow albedo, and snow cover fraction that are not validated in the model.

The model performance with the new LI and SI is described by calculating the root mean square errors (RMSEs) of albedo with observation as shown in Fig. 5. The performance of the Noah-MP in calculating albedo has greatly improved – RMSE is reduced by approximately 73 %. Although we optimized SI with the MTSA, Fig. 5 shows how the parameterization affects albedo with other options as well. The simulations of albedo are improved for all two-stream radiation transfer and snow surface albedo schemes – BATS (Fig. 5a) and CLASS (Fig. 5b) with RMSEs reduced by approximately 70 % on the average. Albedo with other radiation option is also overestimated due to unrealistic leaf and stem effect. Thus, the optimal LI and SI with the MTSA have the similar effect on albedo calculated with other options. The RMSEs with the original minimum values of LAI and SAI increase until the mid winter (e.g., the 17th Julian day) and decrease after that. During the winter, albedo is dominantly influenced by the snow cover and forest masking (Bonan, 2008; Essery et al., 2009; Brovkin et al., 2013). The Noah-MP overestimates snow cover fraction and underestimates vegetation parameters (i.e., LAI and SAI) related to albedo, therefore it makes albedo be greatly overestimated. This error is significantly reduced by applying new parameters that consider all the forest structure effect with realistic values.

4 Conclusions

In winter, albedo has a large variation due to snow cover; however, in the forest region, the snow-covered albedo remains low because of two reasons. First, when the snow covers a forest canopy, the incident radiation is diffused rather than reflected due to irregular surfaces. Second, vegetation shields the snow-covered surfaces. In addition, under the forest, temperature is relatively high and snow tends to melt earlier. This effect reduces albedo further, causing more radiation to be absorbed by the ground; thus resulting in a strong positive feedback (Qu and Hall, 2007). Therefore, accurate calculation of albedo is very influential in the land surface processes. We have addressed the noticeable relationship between the vegetation types and the snow surface albedo through satellite observations. Nevertheless, in the Noah land surface model with multiple physics options (Noah-MP) as well as many land surface models, albedo was calculated without considering the vegetation effects properly. In order to apply the vegetation effect on the snow-covered albedo, we have introduced new parameters, called leaf index (LI) and stem index (SI). We focused on the SI effect because stems are more critical than leaves in the winter albedo. The performance of the Noah-MP in calculating albedo has remarkably improved with simple parameterization for all radiation options and snow surface albedo schemes. However, there is a limitation to enhancing the accuracy of albedo by changing only vegetation indices. Thus, it is required to assess the other parameters, too, such as snow cover fraction and fresh snow albedo, which are not validated against observations.

Acknowledgements. This work is supported by the National Research Foundation of Korea grant (No. 2009-0083527) funded by the Korean government (MSIP). The authors thank Seungbum Hong at the National Institute of Ecology, Korea, for assistance with the Noah-MP.

References

Anderson, J. R.: A Land Use and Land Cover Classification System for Use With Remote Sensor Data, Vol. 964, US Government Printing Office, Washington, 1976.

Asner, G. P., Scurlock, J. M., and Hicke, J. A.: Global synthesis of leaf area index observations: implications for ecological and remote sensing studies, Global Ecol. Biogeogr., 12, 191–205, 2003.

Bonan, G. B.: Forests and climate change: forcings, feedbacks, and the climate benefits of forests, Science, 320, 1444–1449, 2008.

Brovkin, V., Boysen, L., Raddatz, T., Gayler, V., Loew, A., and Claussen, M.: Evaluation of vegetation cover and land-surface albedo in MPI-ESM CMIP5 simulations, J. Adv. Model. Earth Syst., 5, 48–57, doi:10.1029/2012MS000169, 2013.

Cescatti, A., Marcolla, B., Vannan, S. K. S., Pan, J. Y., Roman, M. O., Yang, X., Ciais, P., Cook, R. B., Law, B. E., Matteucci, G., Migliavacca, M., Moors, E., Richardson, A. D., Seufert, G., and Schaaf, C. B.: Intercomparison of MODIS albedo retrievals and in situ measurements across the global FLUXNET network, Remote Sens. Environ., 121, 323–334, 2012.

Dickinson, R. E., Henderson-Sellers, A., and Kennedy, P. J.: Biosphere–Atmosphere Transfer Scheme (BATS) version 1e as coupled to the NCAR Community Climate Model, NCAR Tech. Note NCAR/TN-387+STR, Natl. Cent. for Atmos. Res., Boulder, CO, 80 pp., 1993.

Essery, R., Rutter, N., Pomeroy, J., Baxter, R., Stahli, M., Gustafsson, D., Barr, A., Bartlett, P., and Elder, K.: An evaluation of forest snow process simulations, B. Am. Meteorol. Soc., 90, 1120–1135, 2009.

GMDD
8, 3197–3218, 2015

Gao, F., Schaaf, C. B., Strahler, A. H., Roesch, A., Lucht, W., and Dickinson, R.: MODIS bidirectional reflectance distribution function and albedo Climate Modeling Grid products and the variability of albedo for major global vegetation types, J. Geophys. Res., 110, D01104, doi:10.1029/2004JD005190, 2005.

Henderson-Sellers, A. and Wilson, M. F.: Surface albedo data for climatic modeling, Rev. Geophys., 21, 1743–1778, doi:10.1029/RG021i008p01743, 1983.

Jin, Y., Schaaf, C. B., Gao, F., Li, X., Strahler, A. H., Zeng, X., and Dickinson, R. E.: How does snow impact the albedo of vegetated land surfaces as analyzed with MODIS data?, J. Geophys. Res., 29, 12.1–12.4, doi:10.1029/2001GL014132, 2002.

Leonard, R. E. and Eschner, A. R.: Albedo of intercepted snow, Water Resour. Res., 4, 931–935, doi:10.1029/WR004i005p00931, 1968.

Niu, G.-Y. and Yang, W.-L.: Effects of vegetation canopy processes on snow surface energy and mass balances, J. Geophys. Res., 109, D23111, doi:10.1029/2004JD004884, 2004.

Niu, G.-Y. and Yang, Z.-L.: An observation-based formulation of snow cover fraction and its evaluation over large North American river basins, J. Geophys. Res., 112, D21101, doi:10.1029/2007JD008674, 2007.

Niu, G.-Y., Yang, Z.-L., Mitchell, K. E., Chen, F., Ek, M. B., Barlage, M., Kumar, A., Manning, K., Niyogi, D., Rosero, E., Tewari, M., and Xia, Y.: The community Noah land surface model with multiparameterization options (Noah-MP): 1. model description and evaluation with local-scale measurements, J. Geophys. Res., 116, D12109, doi:10.1029/2010JD015139, 2011.

Norman, J. R.: Microclimate: The Biological Environment, John Wiley, Canada, 1983.

Qu, X. and Hall, A.: What controls the strength of snow-albedo feedback?, J. Climate, 20, 3971–3981, doi:10.1175/JCLI4186.1, 2007.

Rodell, M., Houser, P. R., Jambor, U., Gottschalck, J., Mitchell, K., Meng, C- J., Arsenault, K., Cosgrove, B., Radakovich, J., Bosilovich, M., Entin, J. K., Walker, J. P., Lohmann, D., and Toll, D.: The Global Land Data Assimilation System, B. Am. Meteorol. Soc., 85, 381–394, doi:10.1175/BAMS-85-3-381, 2004.

Schaaf, C. B., Gao, F., Strahler, A. H., Lucht, W., Li, X., Tsang, T., Strugnell, N. C., Zhang, X., Jina, Y., Muller, J.-P., Lewis, P., Barnsley, M., Hobson, P., Disney, M., Roberts, G., Dunderdale, M., Doll, C., d'Entremont, R. P., Hu, B., Liang, S., Privette, J. L., and Roy, D.: First operational BRDF, albedo nadir reflectance products from MODIS, Remote Sens. Environ., 83, 135–148, 2002.

GMDD
8, 3197–3218, 2015

Representation of vegetation effects on the snow-covered albedo

S. Park and S. K. Park

Title Page
Abstract Introduction
Conclusions References
Tables Figures
◂ ▸
Back Close
Full Screen / Esc
Printer-friendly Version
Interactive Discussion

Sellers, P. J.: Canopy reflectance, photosynthesis and transpiration, Int. J. Remote Sens., 6, 1335–1372, 1985.

Tian, Y., Dickinson, R. E., Zhou, L., Zeng, X., Dai, Y., Myneni, R. B., Knyazikhin, Y., Zhang, X., Friedl, M., Yu, H., Wu, W., and Shaikh, M.: Comparison of seasonal and spatial variations of leaf area index and fraction of absorbed photosynthetically active radiation from Moderate Resolution Imaging Spectroradiometer (MODIS) and Common Land Model, J. Geophys. Res., 109, D01103, doi:10.1029/2003JD003777, 2004.

Verseghy, D. L.: CLASS-A Canadian land surface scheme for GCMS: I. Soil model, Int. J. Climatol., 11, 111–133, doi:10.1002/joc.3370110202, 1991.

Wang, Z. and Zeng, X.: Evaluation of snow albedo in land models for weather and climate studies, J. Clim. Appl. Meteorol., 49, 363–380, 2010.

Yang, Z.-L. and Dickinson, R. E.: Validation of the snow submodel of the Biosphere–atmosphere transfer scheme with Russian snow cover and meteorological observation data, J. Climate, 10, 353–373, 1997.

Yang, Z.-L., Niu, G.-Y., Mitchell, K. E., Chen, F., Ek, M. B., Barlage, M., Longuevergne, L., Manning, K., Niyogi, D., Tewari, M., and Xia, Y.: The community Noah land surface model with multiparameterization options (Noah-MP): 2. Evaluation over global river basins, J. Geophys. Res., 116, D12110, doi:10.1029/2010JD015140, 2011.

GMDD

8, 3197–3218, 2015

Representation of vegetation effects on the snow-covered albedo

S. Park and S. K. Park

Table 1. The USGS land cover classification.

USGS land cover type	
1-Urban and Built-up Land	15-Mixed Forest
2-Dryland Cropland and Pasture	16-Water bodies
3-Irrigated Cropland and Pasture	17-Herbaceous Wetland
4-Mixed Dryland/Irrigated Cropland and Pasture	18-Wooded Wetland
5-Cropland/Grassland Mosaic	19-Barren or Sparsely Vegetated
6-Cropland/Woodland Mosaic	20-Herbaceous Tundra
7-Grassland	21-Wooded Tundra
8-Shrubland	22-Mixed Tundra
9-Mixed Shrubland/Grassland	23-Bare Ground Tundra
10-Savanna	24-Snow or Ice
11-Deciduous Broadleaf Forest	25-Playa
12-Deciduous Needleleaf Forest	26-Lava
13-Evergreen Broadleaf Forest	27-White Sand
14-Evergreen Needleleaf Forest	

GMDD
8, 3197–3218, 2015

Representation of vegetation effects on the snow-covered albedo

S. Park and S. K. Park

Table 2. Geographic location, vegetation type and percentage of dominant vegetation type for selected areas.

Area	Longitude	Latitude	Vegetation type	Percentage
(1)	105.00–107.25° E	56.50–58.25° N	Mixed Forest	71.4
(2)	116.25–120.00° E	55.50–57.75° N	Shrubland Mixed Shrubland/Grassland	80.0
(3)	122.50–127.75° E	57.50–60.00° N	Deciduous Needleleaf Forest	85.7
(4)	133.75–136.50° E	55.75–60.00° N	Deciduous Needleleaf Forest	90.4
(5)	138.50–140.75° E	56.25–60.00° N	Shrubland Mixed Shrubland/Grassland	82.6
(6)	121.25–126.50° E	53.75–55.75° N	Deciduous Needleleaf Forest	93.5
(7)	107.75–111.50° E	49.00–51.00° N	Mixed Forest	81.7
(8)	113.75–117.75° E	45.00–49.00° N	Grassland	97.2
(9)	123.75–127.75° E	46.75–50.25° N	Dryland Cropland and Pasture	77.2
(10)	135.00–137.75° E	45.00–47.74° N	Mixed Forest	93.8

GMDD
8, 3197–3218, 2015

Table 3. Minimum value of LAI, reference values (LI), the default minimum value of SAI, and optimized SI values for selected USGS land cover type (forest). The optimized values are based on the sensitivity test.

USGS Land Cover type	Minimum of LAI (default)	LI (reference)	Minimum of SAI (default)	SI (optimized)
11-Deciduous Broadleaf Forest	0.05	0.6	0.01	1.3
12-Deciduous Needleleaf Forest	0.05	0.5	0.01	1.5
14-Evergreen Needleleaf Forest	0.05	0.5	0.01	2.3
15-Mixed Forest	0.05	0.5	0.01	2.0

GMDD
8, 3197–3218, 2015

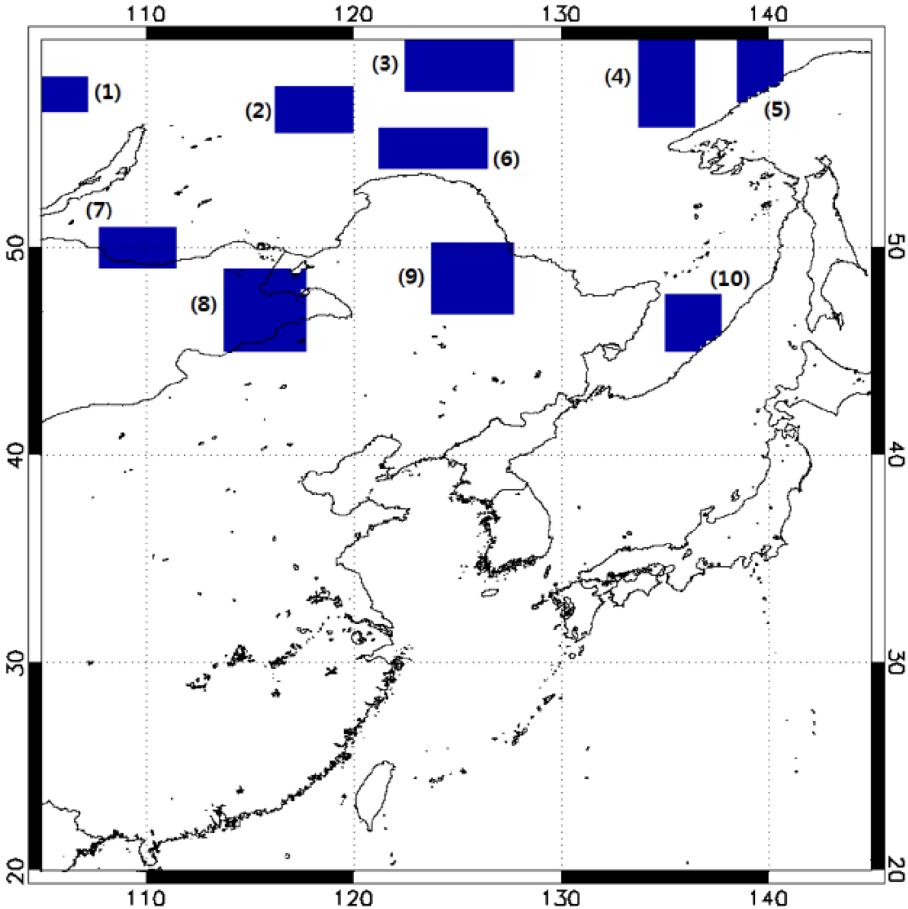

Figure 1. Geographical locations of the study domain.

GMDD
8, 3197–3218, 2015

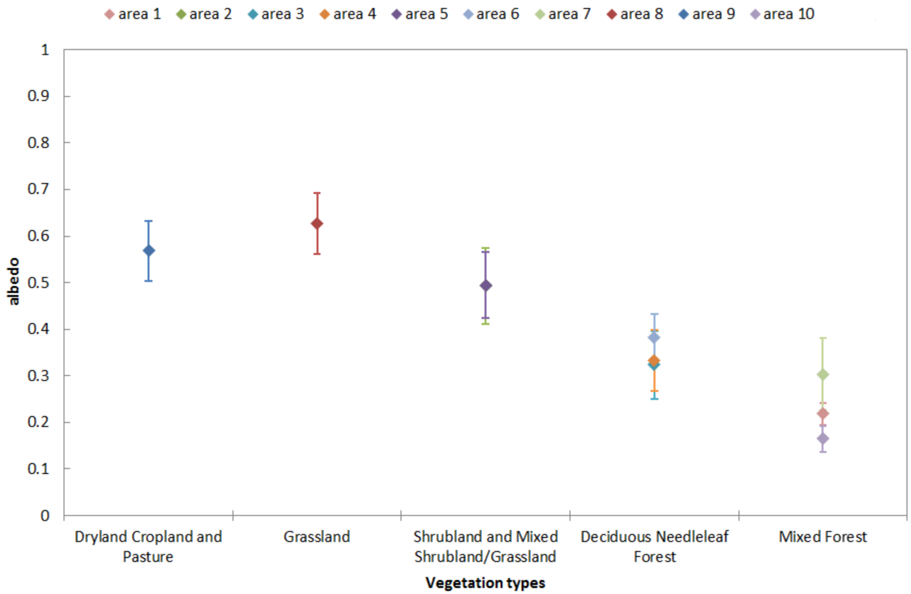

Figure 2. The white-sky albedo for total shortwave broadband averaged for winter time in 2001–2010 (dots) and corresponding SD (bars) when SCF equals 100 %.

GMDD
8, 3197–3218, 2015

Representation of vegetation effects on the snow-covered albedo

S. Park and S. K. Park

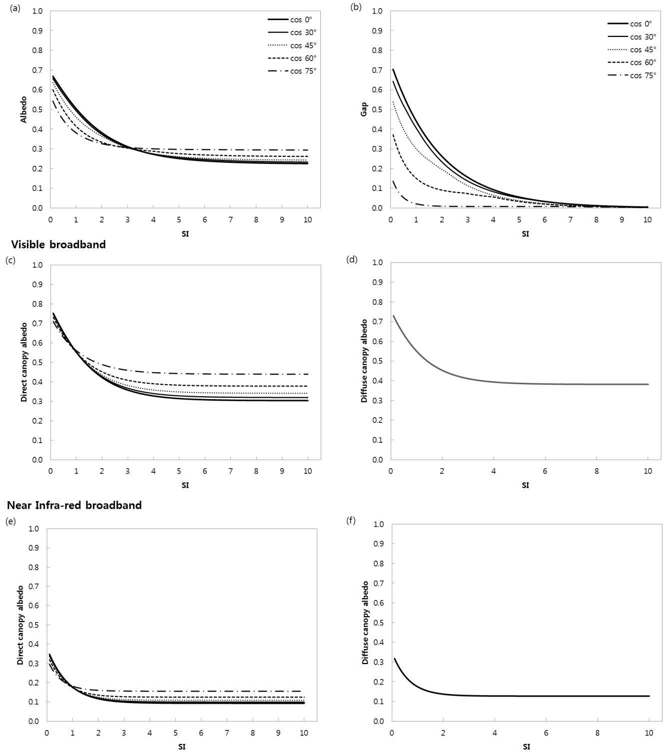

Figure 3. Sensitivity of the snow-covered surface albedo and each term in the albedo equation in the Noah-MP to SI averaged over four forest types: **(a)** total albedo, **(b)** canopy gap probability, **(c)** direct albedo and **(d)** diffuse albedo for visible broadband, and **(e)** direct albedo and **(f)** diffuse albedo for near-infrared broadband.

GMDD
8, 3197–3218, 2015

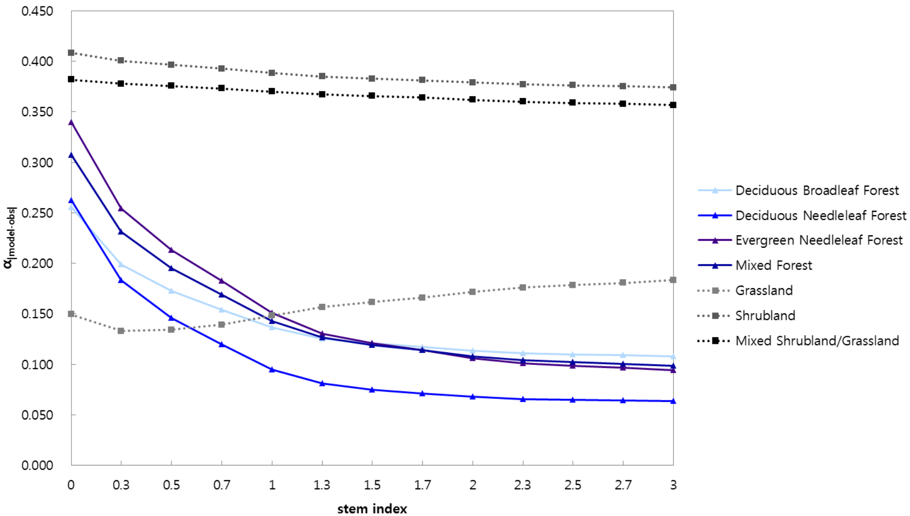

Figure 4. Sensitivity of the winter-averaged albedo to SI over four forest types and three short vegetation types in the Noah-MP for 2001–2010.

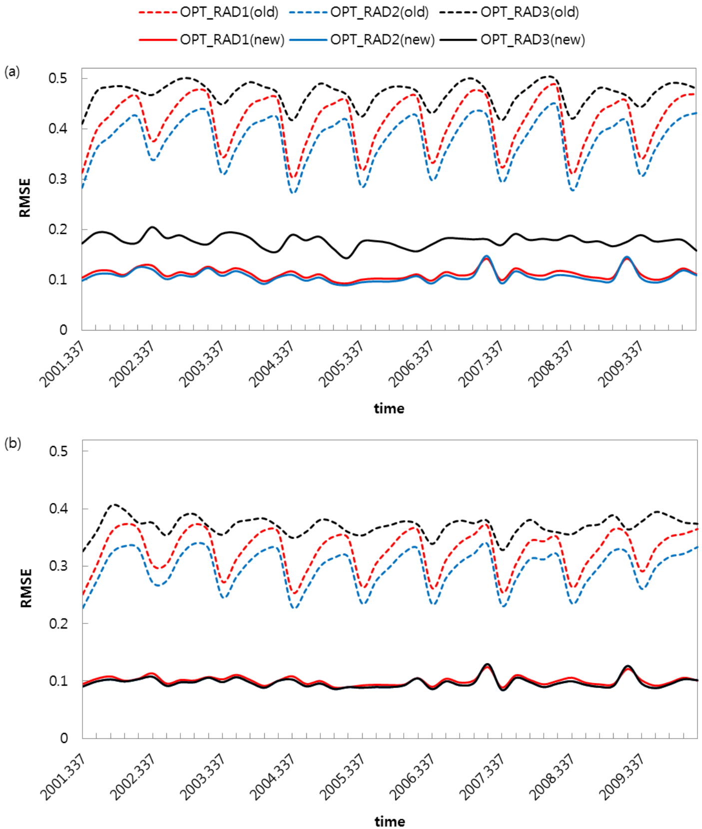

Figure 5. Comparison of RMSE values of albedo with the original minimum value of LAI and SAI (dashed lines) vs. new LI and SI (solid lines) for three radiation options for **(a)** BATS and **(b)** CLASS.

GMDD
8, 3197–3218, 2015

Representation of vegetation effects on the snow-covered albedo

S. Park and S. K. Park